Supporting Information

Fluorescence 'on-off-on' chemosensor for the sequential recognition of Hg^{2+} and Cys in water

Ye Won Choi, Jae Jun Lee, Ga Rim You, Cheal Kim*

Department of Fine Chemistry and Department of Interdisciplinary Bio IT Materials, Seoul National University of Science and Technology, Seoul 139-743, Korea. Fax: +82-2-973-9149; Tel: +82-2-970-6693; E-mail:chealkim@seoultech.ac.kr

Table S1. Examples for the sequential detection of Hg^{2+} and Cys by organic chemosensors

Sensor	Detection Limit (μM)	Interference	Percent of water in solution	Method of detection	Analyte	Reference
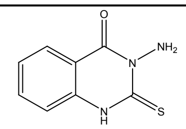	0.35	No data	90%	Fluorescence	Cys	59
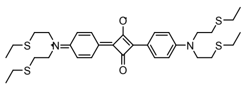	No data	No data	33.3%	Fluorescence UV-vis	Cys, Hcy, GSH, His	60
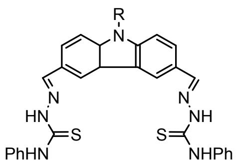	9.6×10^{-5}	None	99%	Fluorescence	Cys	61
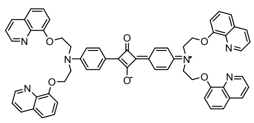	0.037	None	70%	Fluorescence UV-vis	Cys	62
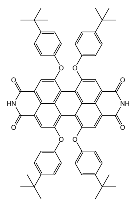	0.091	None	33.3%	Fluorescence UV-vis	Cys	63
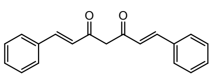	1.0	None	30%	Fluorescence UV-vis	Cys	64
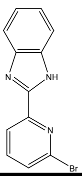	5.2	None	99%	Fluorescence	Cys	This work

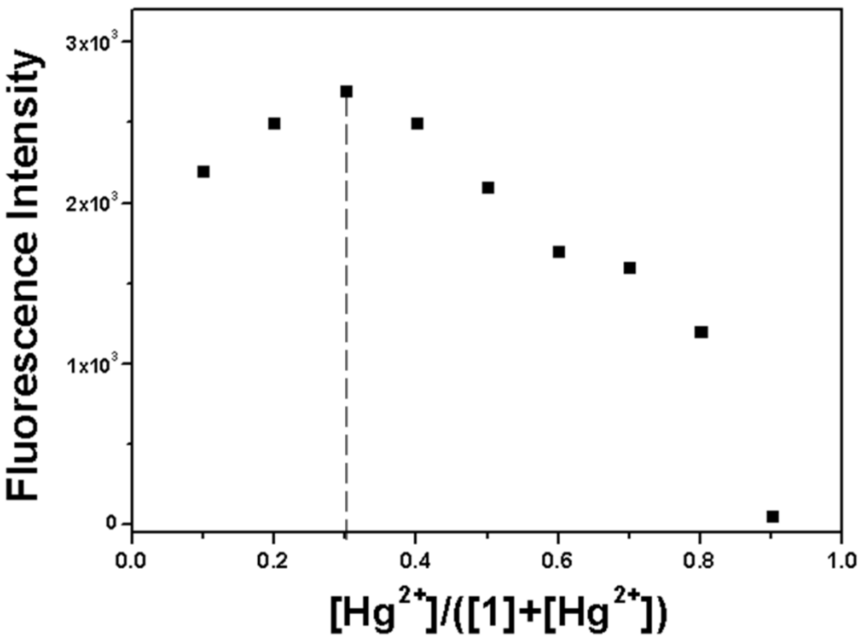

Fig. S1 Job plot of **1** and Hg^{2+} in bis-tris buffer solution (10 mM, pH 7.0). The total concentrations of **1** and Hg^{2+} were 100 μM.

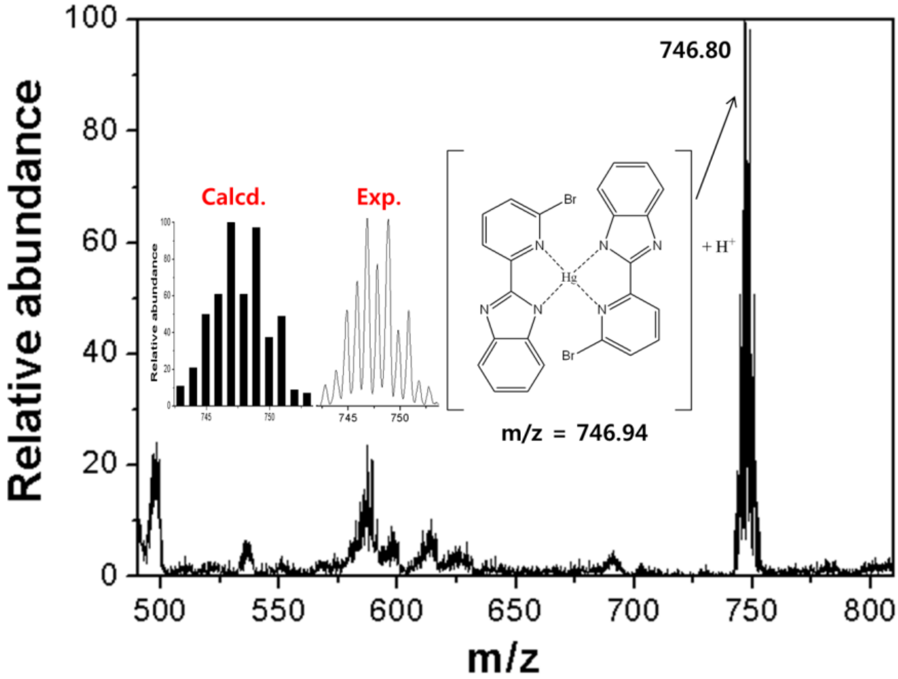

Fig. S2 Positive-ion electrospray ionization mass spectrum of **1** (100 μM) upon addition of 0.5 equiv of $Hg(NO_3)_2$.

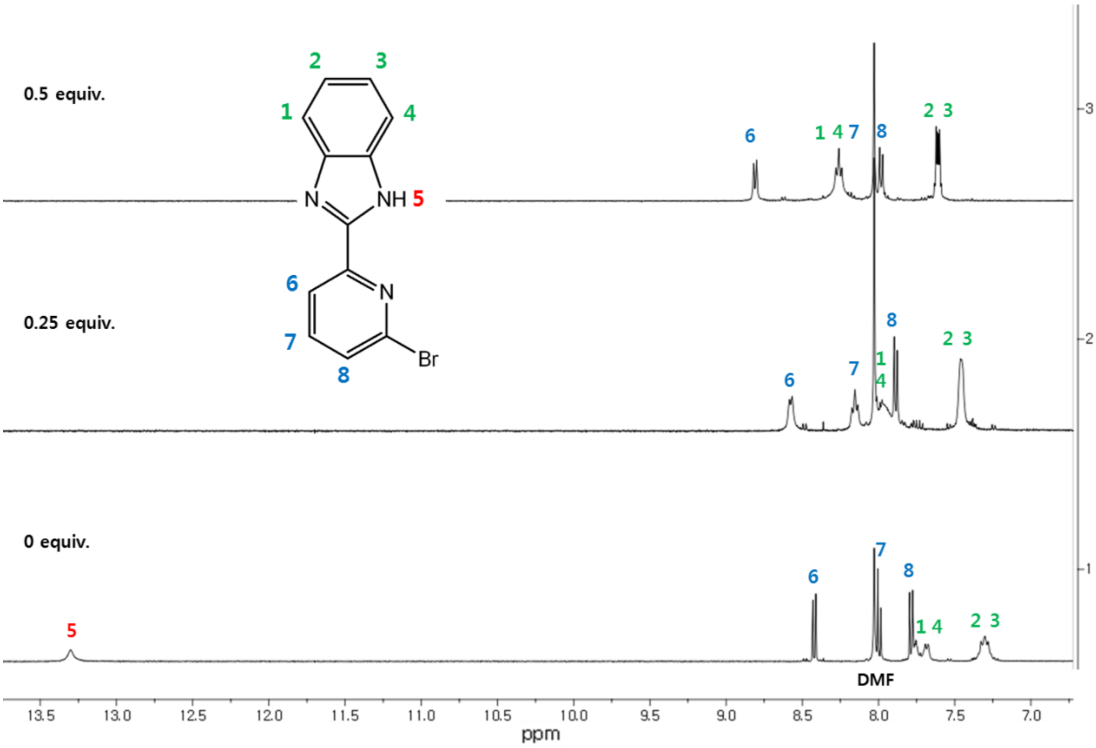

Fig. S3 ^{1}H NMR titration of **1** with Hg^{2+}.

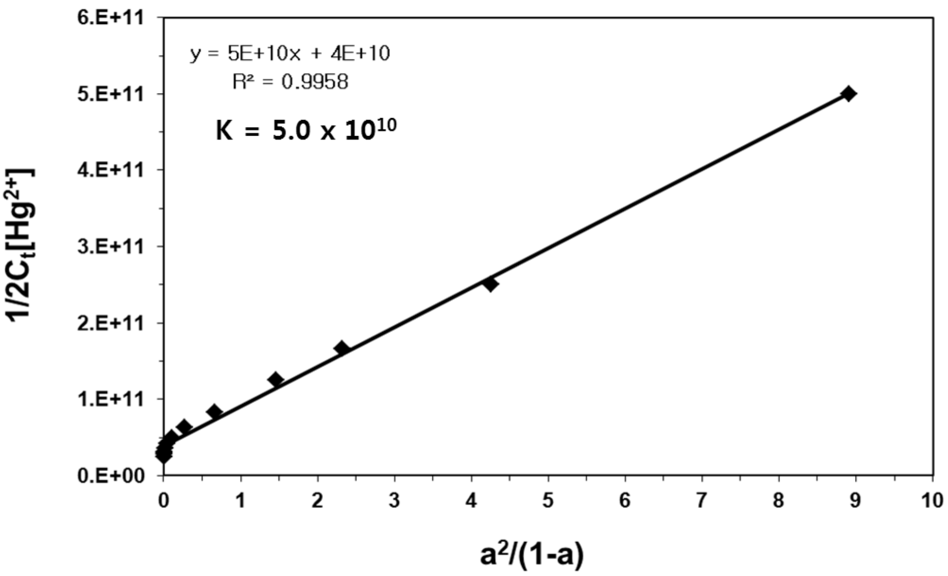

Fig. S4 Li's equation of **1** (at 395 nm), assuming 1:2 stoichiometry for association between Hg^{2+} and **1**.

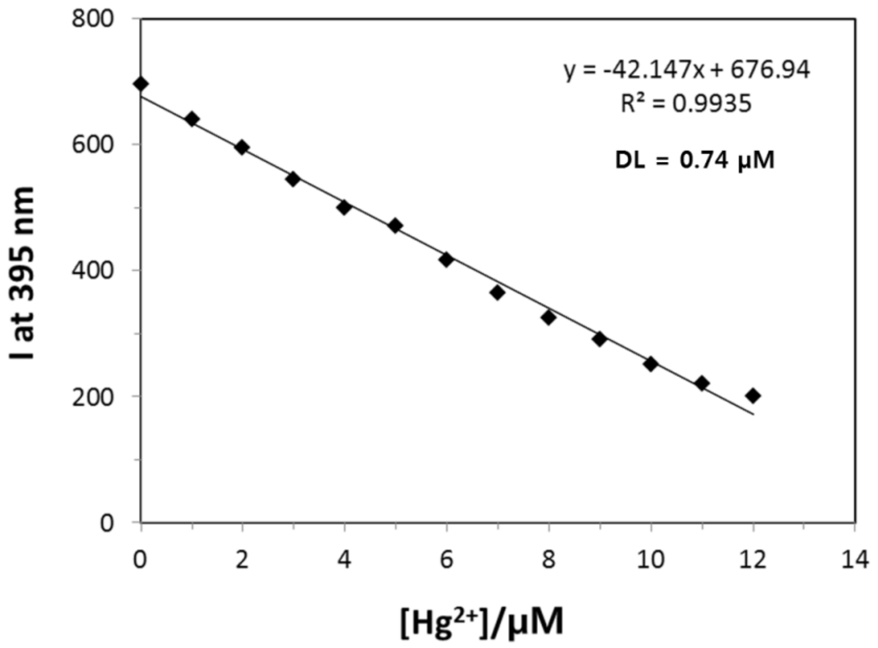

Fig. S5 Detection limit of **1** (1 μM) for Hg^{2+} through change of fluorescence intensity.

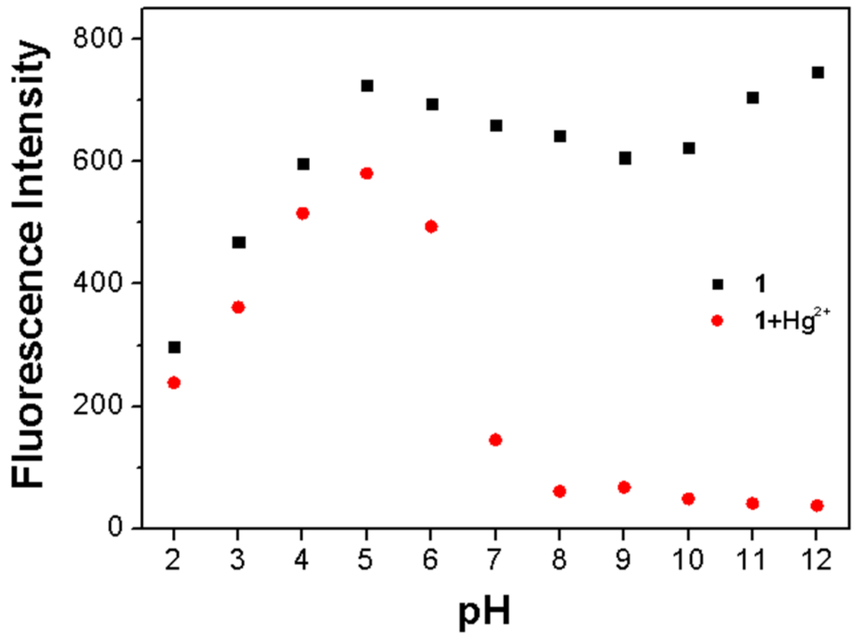

Fig. S6 Fluorescence intensities of **1** upon addition of 25 equiv of Hg^{2+} at various range of pH.

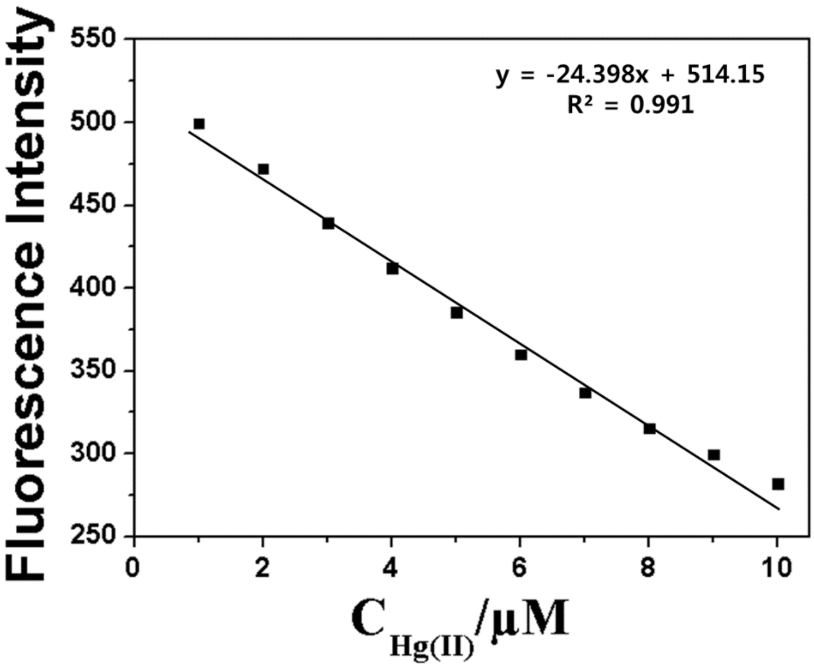

Fig. S7 Fluorescence intensity (at 395 nm) of **1** as a function of Hg^{2+} concentration ([**1**] = 1 μmol/L and [Hg^{2+}] = 1.0-10.0 μmol/L).

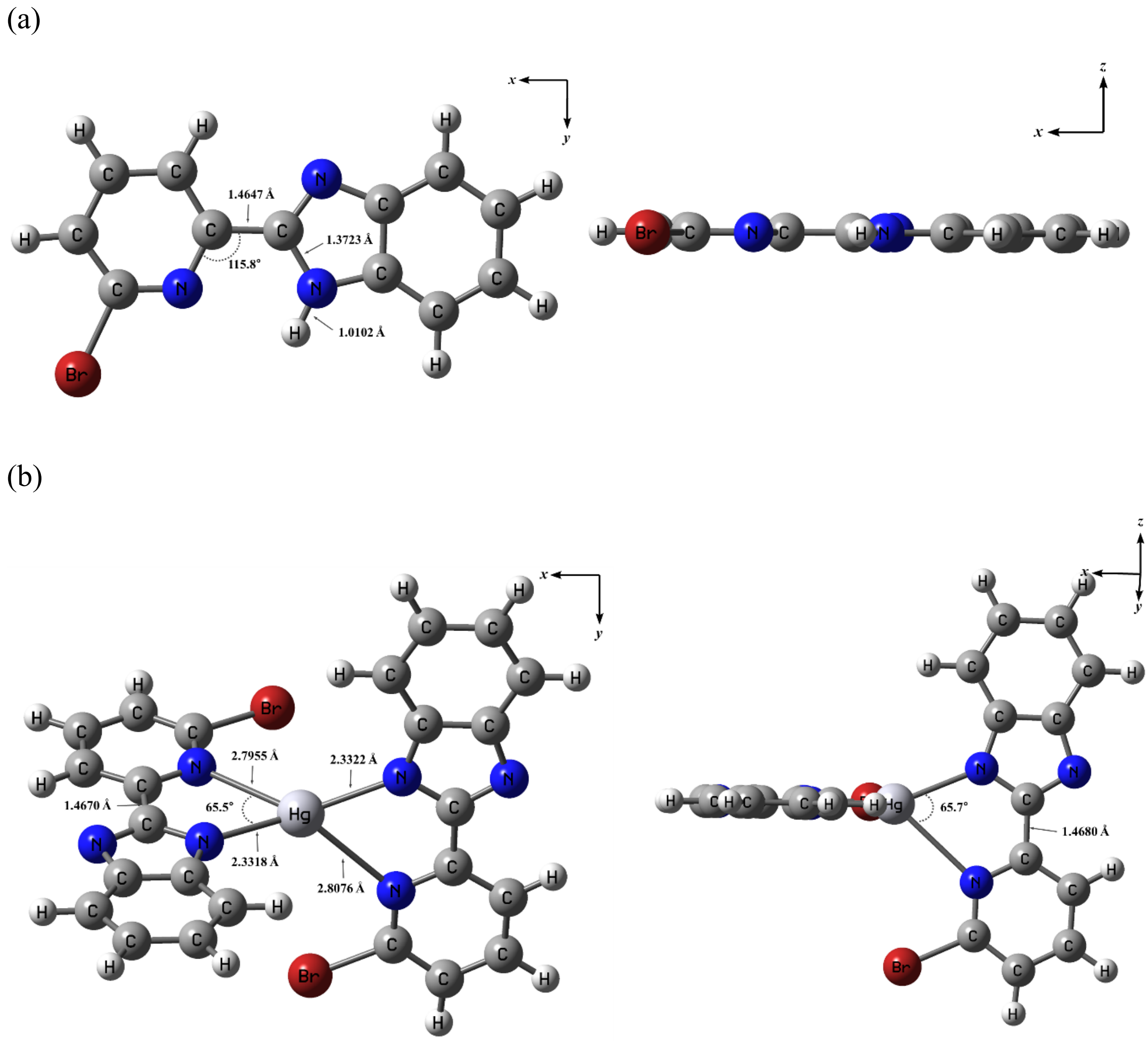

Fig. S8 The energy-minimized structures of (a) **1** and (b) Hg^{2+}-2·**1**.

(a)

Excited State 1	Wavelength	Percent (%)	Oscillator strength
H → L	317.90 nm	96%	0.7856
H-1 → L		2%	
Excited State 2	**Wavelength**	**Percent (%)**	**Oscillator strength**
H-1 → L	307.43 nm	96%	0.0238
H → L		2%	

(b)

Molecular orbital (1)		
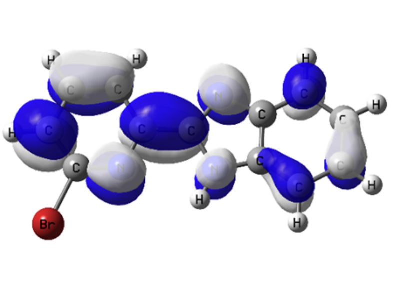	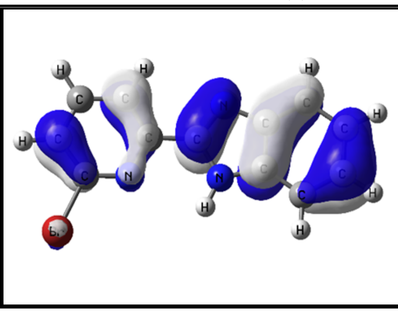	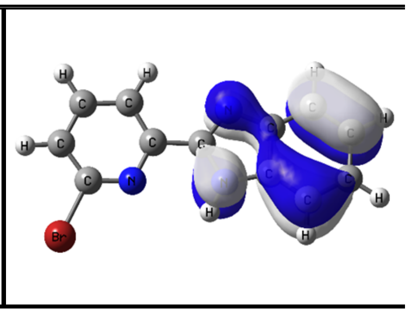
LUMO **(-1.808 eV)**	**HOMO** **(-6.111 eV)**	**LUMO - 1** **(-6.361 eV)**

Fig. S9 (a) The major electronic transition energies and molecular orbital contributions for **1** (H = HOMO and L = LUMO). (b) Isosurface (0.030 electron bohr^{-3}) of molecular orbitals participating in the major singlet excited states of **1**.

(a)

Excited State 1	Wavelength	Percent (%)	Oscillator strength
H-1 → L	342.03 nm	36%	0.4211
H-2 → L		20%	
H-3 → L		11%	
H-3 → L+1		9%	
H-1 → L+1		8%	
H → L		7%	
H → L+1		5%	
Excited State 2	**Wavelength**	**Percent (%)**	**Oscillator strength**
H → L+1	341.05 nm	36%	0.4556
H-2 → L+1		23%	
H-3 → L		14%	
H-1 → L		10%	
H-3 → L+1		8%	
H → L		6%	
Excited State 3	**Wavelength**	**Percent (%)**	**Oscillator strength**
H-1 → L	338.24 nm	33%	0.2312
H-3 → L		28%	
H-2 → L+1		16%	
H → L+1		11%	
H-2 → L		9%	

(b)

Molecular orbital (1-Hg^{2+})		
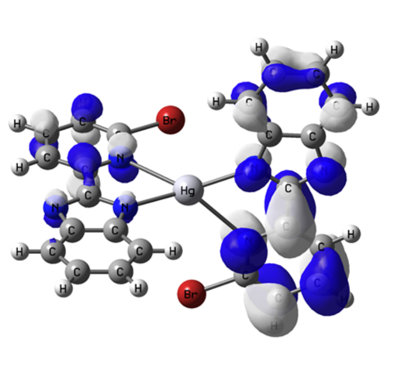	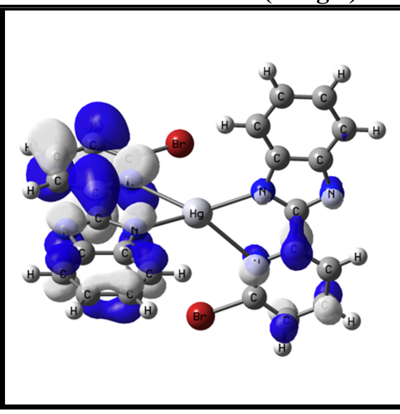	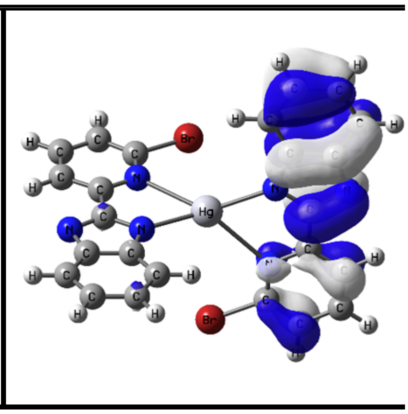
LUMO + 1 **(-1.561 eV)**	**LUMO** **(-1.570 eV)**	**HOMO** **(-5.644 eV)**
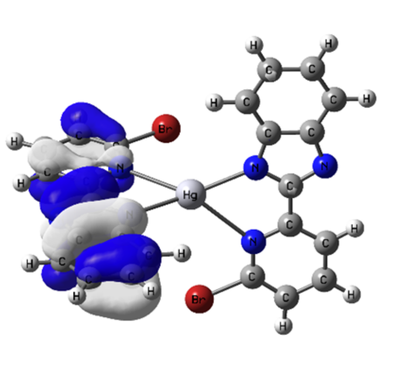	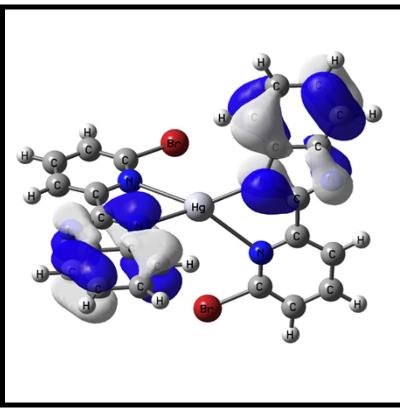	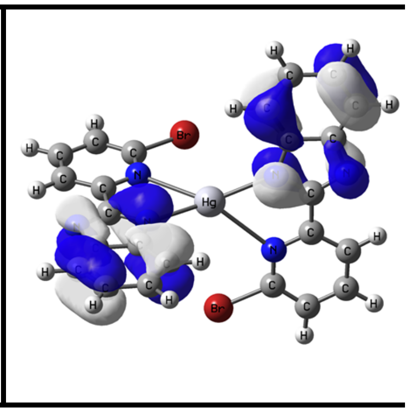
HOMO - 1 **(-5.646 eV)**	**HOMO - 2** **(-5.748 eV)**	**HOMO - 3** **(-5.749 eV)**

Fig. S10 (a) The major electronic transition energies and molecular orbital contributions for Hg^{2+}-2·**1** complex (H = HOMO and L = LUMO). (b) Isosurface (0.030 electron bohr^{-3}) of molecular orbitals participating in the major singlet excited states of Hg^{2+}-2·**1** complex.

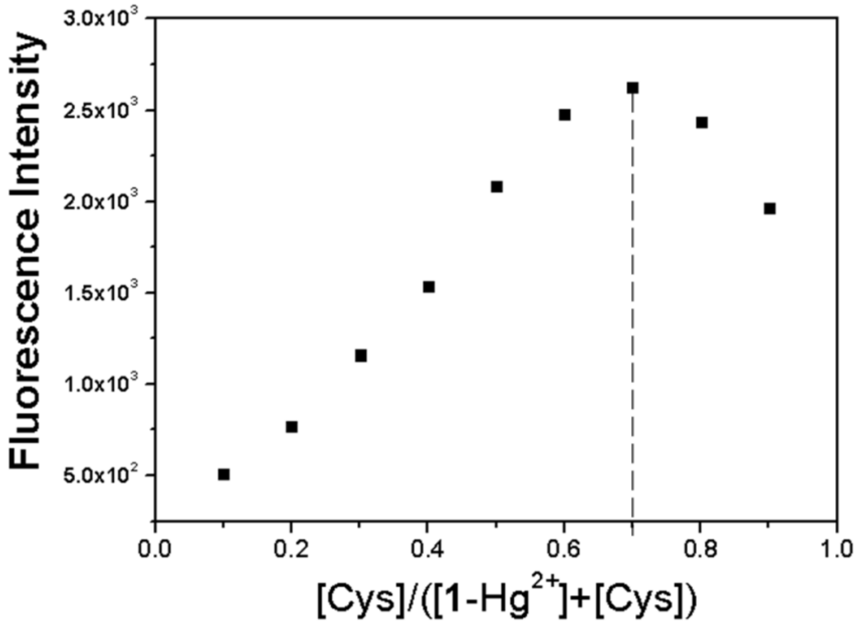

Fig. S11 Job plot of Hg^{2+}-2·**1** and Cys in bis-tris buffer solution (10 mM, pH 7.0). The total concentrations of Hg^{2+}-2·**1** and Cys were 50 μM.

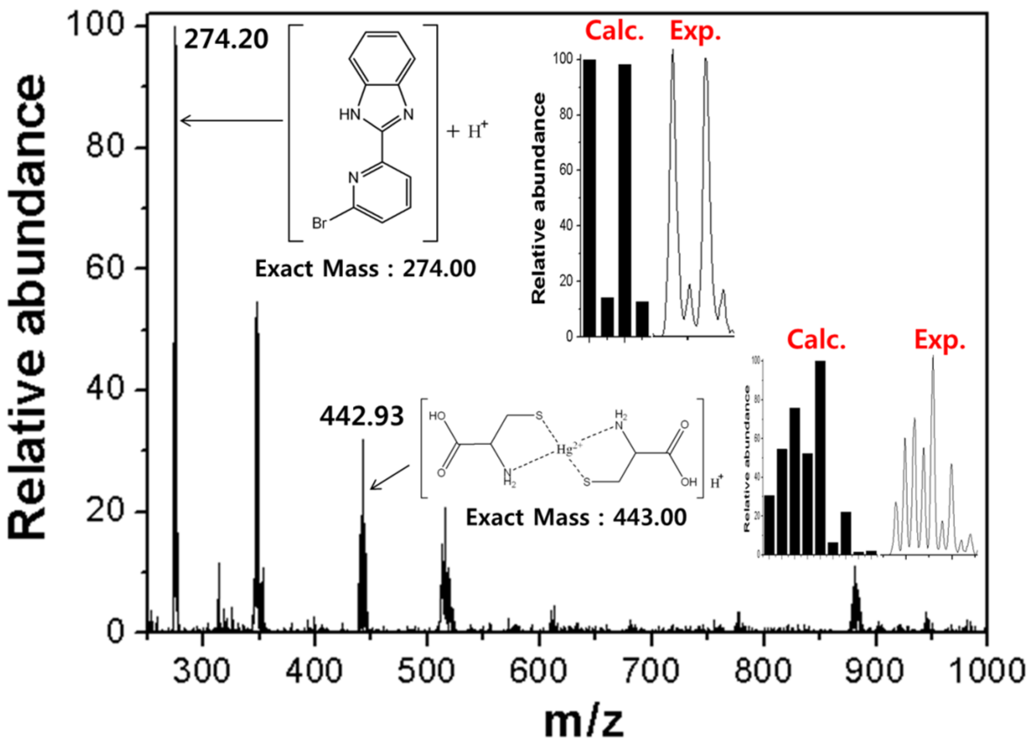

Fig. S12 Positive-ion electrospray ionization mass spectrum of Hg^{2+}-2·**1** (50 μM) upon addition of 2.0 equiv of Cys.

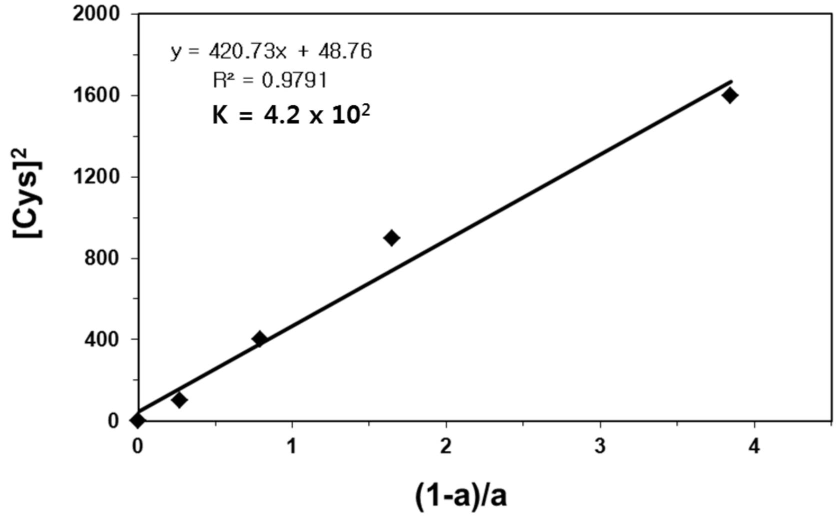

Fig. S13 Li's equation of Hg^{2+}-2·**1** (at 395 nm), assuming 1:2 stoichiometry for association between Hg^{2+}-2·**1** and Cys.

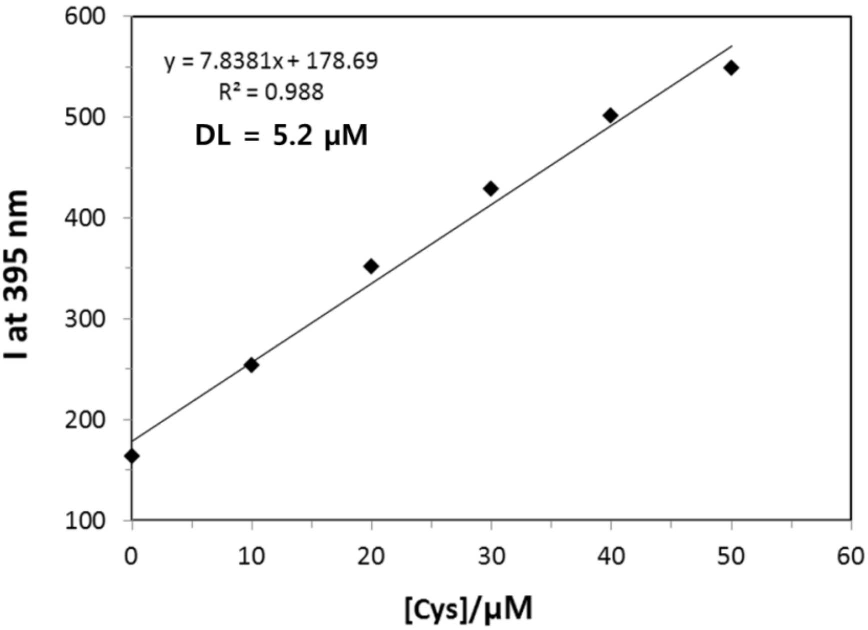

Fig. S14 Detection limit of Hg^{2+}-2·**1** (1 μM) for Cys through change of fluorescence intensity.